August 1995 Chem. Pharm. Bull. 43(8) 1395—1397 (1995) 1395

Solution Forms of Antitumor Cyclic Pentapeptides with 3,4-Dichlorinated Proline Residues, Astins A and C, from *Aster tataricus*[1)]

Hiroshi MORITA, Shinji NAGASHIMA, Koichi TAKEYA, and Hideji ITOKAWA*

Department of Pharmacognosy, School of Pharmacy, Tokyo University of Pharmacy and Life Science, Horinouchi 1432-1, Hachioji, Tokyo 192-03, Japan.

Received March 8, 1995; accepted April 17, 1995

Conformational analysis of antitumor cyclic pentapeptides, astins A (1) and C (3), was made by a combination of NMR and computational techniques. These results indicated that the backbone conformations of 1 and 3, with lower activity than astin B (2), were different from that of 2. The backbone conformation together with a *cis* 3,4-dichlorinated proline residue was considered to play an important role in the antitumor activities of astins.

Key words conformation; astin A; astin C; antitumor cyclic pentapeptide; 3,4-dichlorinated proline; *Aster tataricus*

On the basis of the existence of many naturally occurring cyclic peptides with unique structures and biological activities, we have focused our attention on new cyclic peptides, with various biological activities, from higher plants.[2)] As part of this program, we have reported on the structures of antitumor cyclic pentapeptides, named astins from the roots of *Aster tataricus* (Compositae).[3)] The major cyclic pentapeptides, astins A (**1**), B (**2**) and C (**3**), contain a 16-membered ring system with a unique 3,4-dichlorinated proline, an *allo* threonine, a serine, a β-phenylalanine and an α-aminobutyric acid. In our previous papers,[4,5)] the solid and solution conformations of astin B (**2**), with the highest activity among astins, were described.

Our continuing research on astins, by spectroscopic analysis such as nuclear Overhauser effect (NOE) and temperature effects on the NH chemical shifts in dimethyl sulfoxide-d_6 (DMSO-d_6), and molecular dynamics simulation, demonstrated that astins A (**1**) and C (**3**) with 3,4-dichlorinated proline residues possessed different solution conformations from that of astin B (**2**) in DMSO-d_6 solution. In addition, their backbone conformations were considered to affect the antitumor activities of astins. This paper deals with conformational analysis of astins A (**1**) and C (**3**) by NMR and computational chemical methods.

Results and Discussion

In order to understand the mechanisms involved in the actions of cyclic peptides and to study the structure–activity relationship, it is necessary to have knowledge of their conformational characteristics. Our previous examination using X-ray, NMR and molecular dynamics (MD) simulation indicated that the conformation of astin B (**2**) in the solution state was, on the whole, homologous to that observed in the solid state.[4)] The conformations of astins A (**1**) and C (**3**), with an α-aminobutyric acid (Abu) at residue 2 and lower activity than astin B (**2**), were examined by the use of NMR and MD simulation, and were compared with that of astin B (**2**).

It has been well documented[6)] that changes in temperature have little effect on the chemical shifts of NH protons which are involved in an intramolecular hydrogen bond or which are otherwise shielded from the medium. It has been observed that exposed hydrogens, which are accessible to the solvent, exhibit a larger temperature coefficient (>4 ppb/T) than do intramolecularly hydrogen-bonded hydrogens (<3 ppb/T). In such a solvent as DMSO-d_6, the temperature effect on NH chemical shifts is often used to identify the external or internal NH orientations.

The temperature dependence of the amide proton chemical shift of **1** and **3** was recorded in 5° intervals over the range 300—330 K in DMSO-d_6, as summarized in Table 1. The $\mathrm{d}\delta/\mathrm{d}T$ of both compounds in DMSO-d_6 were quite similar, suggesting that the same amide protons in **1** and **3** are intramolecularly hydrogen bonded in this solvent. On the other hand, the coefficients in **2** were slightly different from those in **1** and **3**. For compounds **1** and **3**, the $\mathrm{d}\delta/\mathrm{d}T$ of β-Phe^4 was 0.5 and 0.0, respectively, indicating that this proton is indeed involved in a strong intramolecular hydrogen bond in this solvent. The coefficient for **2**, however, was 2.8 ppb/K, showing that this NH proton is involved in a weak intramolecular hydrogen bond. In addition, the coefficients of Ser^3-NH

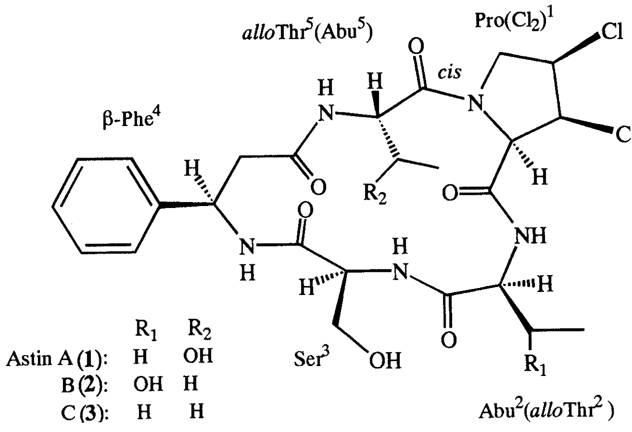

Fig. 1. Structures of Astins A—C

Pro was provisionally numbered as the first amino acid.

Table 1. Temperature Coefficients ($-\mathrm{d}\delta/\mathrm{d}T \times 10^3$ ppm/K) of NH Chemical Shifts of Astins A, B, and C in DMSO-d_6

Compounds	*allo*Thr^2 (Abu^2)	Ser^3	β-Phe^4	Abu^5 (*allo*Thr^5)
Astin A (**1**)	3.5	1.7	0.5	5.3
Astin B (**2**)	3.0	2.2	2.8	4.5
Astin C (**3**)	3.5	1.3	0.0	5.7

---

* To whom correspondence should be addressed.

in **1** and **3** were slightly smaller than that in **2**.

The conformations of **1** and **3**, which were considered to be different from that of **2** by the above temperature coefficients, were deduced from detailed analysis of NOE data in DMSO-d_6. NOE relationships similar to those in **2** were observed in the phase sensitive nuclear Overhauser and exchange spectroscopy (NOESY) spectra,[7)] except that NOEs between Ser^3-H$_\alpha$ and Ser^3-NH, and between Ser^3-NH and Abu^2-Hα were observed in **1** and **3** (Fig. 2). The above NOE relationship was not observed in **2**, because Ser^3-NH was related to the formation of a strong intramolecular hydrogen bond with *allo*Thr^2-OH.

The allowed dihedral angles were calculated from the vicinal NH-C$_\alpha$H coupling constants obtained by ^{1}H-NMR spectra, according to the Karplus type equation proposed by Bystrov *et al.*[8)] The *J* values and the corresponding calculated dihedral angles, ϕ, are shown in Table 2. The corresponding dihedral angles of **1** and **3** have similar values.

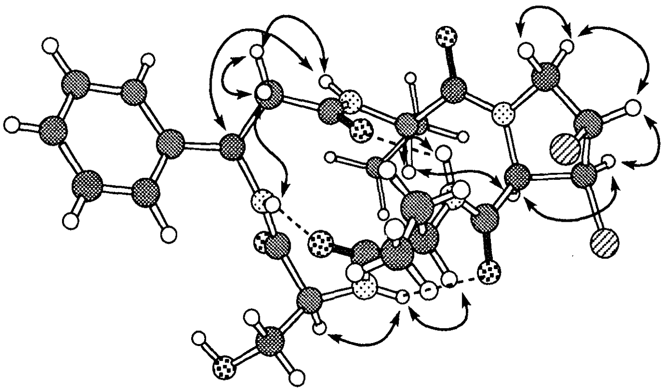

Fig. 2. Some Important NOE Enhancements of Astin C

The arrows show the NOE relationships confirmed by phase sensitive NOESY experiments in DMSO-d_6 at 303 K, and dashed lines show three intramolecular hydrogen bondings.

Table 2. Backbone Dihedrals (ϕ) in Astins A (**1**) and C (**3**), Calculated from Vicinal NH–C$_\alpha$H Coupling Constants (Hz)

Residues	Astin A (**1**)		Astin C (**3**)	
	Hz	ϕ angle[a)]	Hz	ϕ angle[a)]
Abu^2	8.9	−93, 213	9.0	−94, 214
Ser^3	4.6	−68, −172, 17, 103	4.2	−65, −175, 14, 106
β-Phe^4	6.5	−79, −161, 30, 90	6.6	−79, −161, 31, 89
*allo*Thr^5(Abu^5)	6.2	−77, −163, 28, 92	5.1	−71, −169, 20, 100

a) Calculated using the Karplus-Bystrov equation: $^3J_{\mathrm{HN}_\alpha}=9.4\cos^2|60-\phi|-1.1\cos|60-\phi|+0.4$.

In order to characterize the conformational features of astins A and C, restrained molecular dynamics simulation of astin C (**3**) using structural constraints derived from the NMR data was conducted to define the conformation in the same solvent as the NMR experiments. The simulated annealing calculation method,[9)] which we have already reported relating to several cyclic peptides such as surfactin,[10)] astin B[4)] and pseudostellarin A,[11)] was applied to analyzing this problem. The starting coordinates were derived from the X-ray structure of astin B.[5)] The distance constraints derived from the NOE experiments were classified into two ranges, 1.8—2.5 and 1.8—3.5 Å, corresponding to strong and medium NOEs, respectively. No hydrogen bonding restraints and no solvent were used. The *J*-derived ϕ angles were not included in the constraints due to the fact that a coupling constant can correspond to four dihedral angles and the coupling constant could be the result of motional averaging. Each system was equilibrated for 5400 fs with a thermal bath at 500 K, and thereafter successively for 900 fs with a thermal bath 10 K lower in temperature, until a final temperature of 50 K was obtained. This temperature was chosen after several trial and error tests, judging from the arrival at equilibrium between possible conformers. Twenty cycles were performed, and each frozen conformation was sampled from the minimum temperature at 50 K.

Calculated low energy conformers were analyzed in detail and 10 of these conformations have an averaged backbone atom root mean square deviation (RMSD), 0.112 (0.047). A snapshot with the lowest energy was selected as a relevant conformation (Fig. 3). The directions of the amide bond between residues 2 and 3 in **2** and **3** were different from each other, and a superposition of the energy minimized conformers of **2** and **3** is depicted in Fig. 4. The lowest energy conformation of **3**

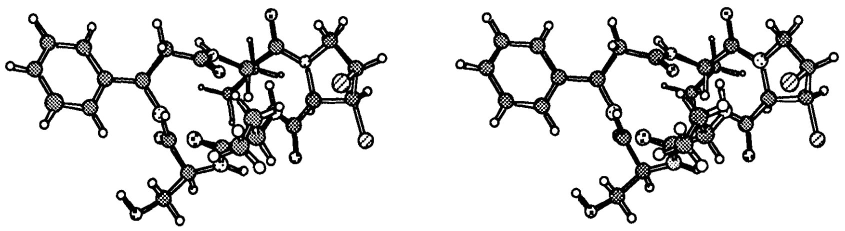

Fig. 3. A Stereoscopic View of the Lowest Energy Conformer of Astin C (**3**) Calculated from Energy Minimizations

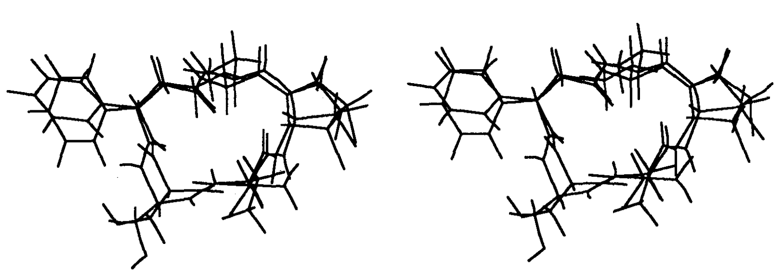

Fig. 4. A Stereo View of a Superposition of the Energy Minimized Conformers of Astins B and C (RMSD=0.62 Å for the Best Fit of Each C$_\alpha$ Carbon)

Table 3. The Calculated Backbone Dihedrals for the Ten Lowest Energy Conformers in Astin C by MD Calculations

Residue	Dihedral angles (S.T.D.) of astin C	
Pro(Cl_2)^1	ϕ	−76.6 (7.7)
	ψ	−8.5 (15.8)
	ω	−176.6 (1.2)
Abu^2	ϕ	−89.3 (17.3)
	ψ	62.1 (3.5)
	ω	−176.6 (1.1)
Ser^3	ϕ	67.9 (2.7)
	ψ	−55.8 (1.4)
	ω	178.1 (0.9)
β-Phe^4	$\phi^{a)}$	−128.8 (5.1)
	$\psi_1{}^{b)}$	46.1 (2.2)
	$\psi_2{}^{b)}$	80.0 (3.0)
	ω	−173.8 (2.0)
Abu^5	ϕ	−67.6 (4.1)
	ψ	142.1 (2.5)
	ω	1.3 (2.3)

a) ϕ in β-Phe^4 = $C_{C=O}$–N–C_β–C_α. *b)* ψ_1 in β-Phe^4 = N–C_β–C_α–$C_{C=O}$, ψ_2 in β-Phe^4 = C_β–C_α–$C_{C=O}$–N.

had three intramolecular hydrogen bonds between Ser^3 and Pro^1 (Ser^3–NH···Pro^1–CO 2.17 Å), between β-Phe^4 and Abu^2 (β-Phe^4–NH···Abu^2–CO 1.77 Å) , and between Abu^2 and β-Phe^4 (Abu^2–NH···β-Phe^4–CO 2.06 Å), which were different from those between Ser^3–NH and *allo*Thr^2–OH, between *allo*Thr^2–NH and β-Phe^4–CO, and between β-Phe^4–NH and β-Phe^4–CO in astin B (**2**). The similarity of this geometry in solution was also investigated by the intensive NOE correlations observed between Ser^3–H_α and Ser^3–NH, and between Ser^3–NH and Abu^2–H_α in **3**, and also by the temperature coefficients of the above three NH protons in **3**. In addition, it is clear from the relevant dihedrals provided in Table 3 that the ϕ angles (Abu^2-94, Ser^3-106, β-Phe^4-161, and *allo*Thr^5-71) roughly correspond with those calculated from the vicinal NH-C_αH coupling constants in the ^{1}H-NMR spectrum (Table 2) and are fulfilled for the solution conformation of **3**. Furthermore, considering the temperature coefficients and NOE relationship, the conformation of astin A (**1**) in DMSO-d_6 was also shown to possess a backbone conformation similar to astin C (**3**).

These results indicated that **1** and **3**, with weaker activity than astin B (**2**), took different backbone conformations from that of **2**. Therefore, the backbone conformation, together with a *cis*-3,4-dichloroproline residue of astins, was considered to play an important role in antitumor activities.

Experimental

All NMR data were recorded on a Bruker AM400 and AM500 and processed on a Bruker data station with an Aspect 3000 computer system. 10 mg samples of astins A and C in a 5 mm tube (0.5 ml DMSO-d_6, degassed) were used for the homonuclear and heteronuclear measurements. The spectra were recorded at 303 K. Phase sensitive NOESY experiments were made with a mixing time of 0.6 s.

Materials Roots of *Aster tataricus* used in this experiment were purchased from Uchida Wakanyaku Co. in Japan, and a voucher specimen has been deposited in the herbarium at the Tokyo University of Pharmacy and Life Science. The extraction and isolation procedures of astins A, B and C were performed as described in our previous paper.[5)]

Simulated Annealing Calculation Computer modeling and all calculations were performed using the molecular-modeling software SYBYL ver. 6.03 (Tripos Associates, St. Louis, MO) on an IRIS 4-D work station. Initial calculations were derived from the coordinates of the crystal structure of astin B analyzed by X-ray crystallography.[4)] The dielectric constant (ε) was assumed to be proportional to the interatomic distances (r) as $\varepsilon = r$. Solvent molecules were not included in the calculations. The NOE relationships shown in Fig. 2 were taken into account in the calculations of the constraint minimizations and dynamics with an extra harmonic term in the form $E = \sum K (r - r_{\max})^2$ for $r > r_{\max}$ and $E = 0.0$ for $r < r_{\max}$ added to the force field. A simulation was performed using a time step of 1 fs, and the structures were sampled every 90 fs. Each system was equilibrated for 5400 fs with a thermal bath at 500 K, and thereafter, successively, for 900 fs with a thermal bath 10 K lower in temperature, until a final temperature of 50 K was obtained. Twenty cycles were performed, giving a total simulation time of 126 ps, and each frozen conformation was sampled from the minimum temperature at 50 K. The snapshots from the minimum temperature at 50 K were then energy minimized with an AMBER force field.[12)] The lowest energy conformer was selected as the relevant conformation. Each energy minimization was carried out until the derivatives became less than 0.01 kcal·mol^{-1}·Å^{-1}.

Acknowledgment The authors thank the Ministry of Education, Science and Culture, Japan, for financial support through Grants-in-Aid for Encouragement of Young Scientists.

References

1) Cyclic Peptides from Higher Plants. Part XX, Part XIX, Morita H., Nagashima S., Takeya K., Itokawa H., *BioMed. Chem. Lett.*, **5**, 677 (1995).

2) Morita H., Yun Y. S., Takeya K., Itokawa H., *Tetrahedron Lett.*, **35**, 9593 (1994), and references cited therein.

3) Morita H., Nagashima S., Takeya K., Itokawa H., *Chem. Pharm. Bull.*, **41**, 992 (1993).

4) Morita H., Nagashima S., Takeya K., Itokawa H., *Tetrahedron*, **50**, 11613 (1994).

5) Morita H., Nagashima S., Takeya K., Itokawa H., Iitaka Y., *Tetrahedron*, **51**, 1121 (1995).

6) Kessler H., *Angew. Chem.*, **94**, 509 (1982); *ibid.*, int. Ed., **21**, 512 (1982).

7) Bodenhauser G., Koger H., Ernst R. R., *J. Magn. Reson.*, **58**, 370 (1984).

8) Bystrov V. F., Ivanov V. T., Portnova S. L., Balashova T. A., Ovchinnikov Yu. A., *Tetrahedron*, **29**, 873 (1973).

9) Wilson S. R., Cui W., Moskowits J., Schmidt K. E., *Tetrahedron Lett.*, **29**, 4373 (1988).

10) Itokawa H., Miyashita T., Morita H., Takeya K., Hirano T., Homma M., Oka K., *Chem. Pharm. Bull.*, **42**, 604 (1994).

11) Morita H., Kayashita T., Takeya K., Itokawa H., *Tetrahedron*, **50**, 12599 (1994).

12) Seibel G., Singh U. C., Weiner P. K., Caldwell J., Kollman P., Univ. California, San Francisco, 1989.